GSK3-β promotes calpain-1–mediated desmin filament depolymerization and myofibril loss in atrophy

Dina Aweida, Inga Rudesky, Alexandra Volodin, Eitan Shimko ⓘ, and Shenhav Cohen ⓘ

Myofibril breakdown is a fundamental cause of muscle wasting and inevitable sequel of aging and disease. We demonstrated that myofibril loss requires depolymerization of the desmin cytoskeleton, which is activated by phosphorylation. Here, we developed a mass spectrometry–based kinase-trap assay and identified glycogen synthase kinase 3-β (GSK3-β) as responsible for desmin phosphorylation. GSK3-β inhibition in mice prevented desmin phosphorylation and depolymerization and blocked atrophy upon fasting or denervation. Desmin was phosphorylated by GSK3-β 3 d after denervation, but depolymerized only 4 d later when cytosolic Ca^{2+} levels rose. Mass spectrometry analysis identified GSK3-β and the Ca^{2+}-specific protease, calpain-1, bound to desmin and catalyzing its disassembly. Consistently, calpain-1 down-regulation prevented loss of phosphorylated desmin and blocked atrophy. Thus, phosphorylation of desmin filaments by GSK3-β is a key molecular event required for calpain-1–mediated depolymerization, and the subsequent myofibril destruction. Consequently, GSK3-β represents a novel drug target to prevent myofibril breakdown and atrophy.

Introduction

Muscle wasting is a debilitating response to denervation, disuse, aging, fasting, and various diseases including motor-neuron diseases (e.g., amyotrophic lateral sclerosis), cancer cachexia, and renal and cardiac failure (Jackman and Kandarian, 2004; Cohen et al., 2015). This loss of mass results largely from the accelerated degradation of the contractile myofibrils, primarily by the ubiquitin-proteasome pathway (Solomon and Goldberg, 1996). Their destruction accounts for the reduction in muscle strength and increased disability that reduce quality of life and contribute to mortality. Two ubiquitin ligases, muscle RING finger 1 (MuRF1) and atrogin-1/MAFbx, are induced in all types of atrophy by forkhead box O (FoxO) transcription factors, and their induction is required to cause wasting (Bodine et al., 2001; Gomes et al., 2001; Sandri et al., 2004). Although much attention has been given to the signaling pathways that promote atrophy, the precise mechanism of myofibril disassembly and the critical specific steps that promote its destruction remain largely unknown. We have shown that myofibril breakdown during atrophy is an ordered process requiring the initial depolymerization of the desmin cytoskeleton (Volodin et al., 2017).

Desmin intermediate filaments are important for maintenance of muscle architecture and function (Chou et al., 2009; Dechat et al., 2009; Mendez et al., 2010), because they link adjacent myofibrils laterally and to the muscle membrane, mitochondria, and nucleus (Lazarides and Hubbard, 1976; Lazarides, 1978).

Mutations in desmin or its deficiency result in disorganized myofibrils (Milner et al., 1996) and cardiomyopathies (Mavroidis et al., 2008), indicating that intact desmin filaments are important for myofibril integrity. Desmin consists of a central α-helical rod domain flanked by non–α-helical amino-terminal head and carboxy-terminal tail domains (Geisler and Weber, 1982). The head domain is important for desmin filament stability and polymerization (Kaufmann et al., 1985), and phosphorylation within this domain promotes desmin disassembly (Inagaki et al., 1987). We and others have shown, that during atrophy induced by denervation or fasting, phosphorylation of desmin on three serine residues within the head domain promotes its ubiquitination by Trim32, disassembly, and degradation (Cohen et al., 2012; Volodin et al., 2017). Because loss of desmin filaments and the attached myofibrils is activated by desmin phosphorylation, inhibition of the critical kinase responsible for this phosphorylation is likely to be of major therapeutic benefit to prevent atrophy in various catabolic states. The present studies were undertaken to identify the kinase responsible for desmin phosphorylation during atrophy in vivo.

These studies have identified glycogen synthase kinase 3-β (GSK3-β) as the kinase promoting desmin filament phosphorylation and subsequent loss during atrophy. This enzyme and its close homologue GSK3-α are ubiquitously expressed serine/threonine kinases, which were originally identified for their key role

Faculty of Biology, Technion Institute of Technology, Haifa, Israel.

Correspondence to Shenhav Cohen: shenhavc@technion.ac.il.

in regulating insulin-stimulated glycogen synthesis (Frame and Cohen, 2001; Doble and Woodgett, 2003; Jope and Johnson, 2004). In addition to this role, GSK3 also regulates gene transcription, protein synthesis, and cytoskeletal organization (Woodgett, 1994; Doble and Woodgett, 2003; Albrecht et al., 2015). In mammalian cells, these two isoforms are encoded by two separate genes and show no functional redundancy, as GSK3-β null mutation in mice is lethal (Hoeflich et al., 2000). By promoting protein phosphorylation that often leads to degradation, GSK3-β regulates signaling pathways (e.g., Wnt and Hedgehog) that control development, cell survival, and tissue homeostasis (Quélo et al., 2004; Viatour et al., 2004; Boucher et al., 2006). One of its bona fide substrates is β-catenin, a component of adhesion complexes and the main effector of Wnt signaling (Valenta et al., 2012), whose phosphorylation by GSK-3β promotes degradation via the proteasome (Stamos and Weis, 2013). We show here that GSK-3β is of prime importance in regulating muscle size because it phosphorylates desmin filaments and promotes their loss, which triggers myofibril destruction and atrophy. A similar role for GSK-3β in the phosphorylation and dissociation of desmin filaments has been recently suggested in failing hearts of mongrel dogs (Agnetti et al., 2014). In normal muscle, this enzyme is inhibited via phosphorylation by PI3K–Akt–FoxO signaling; however, during fasting and in disease states, when IGF-I and insulin levels are low, PI3K–Akt–FoxO signaling decreases, and GSK-3β is activated and catalyzes protein phosphorylation. Although phosphorylation of desmin filaments increases rapidly after denervation of mouse muscle, their dissociation occurs only several days later (Volodin et al., 2017). Thus, depolymerization of phosphorylated desmin filaments probably requires the activation of additional factors, such as calpain-1, as demonstrated here.

Calpain-1 is a member of the Ca^{2+}-activated cysteine proteases (calpains), which play important roles in cell motility, cell proliferation, and apoptosis (Goll et al., 2003). Prior studies in vitro and on cultured cardiomyocytes have suggested a role for calpains in cytoskeletal rearrangement by promoting the cleavage of desmin and vimentin (Nelson and Traub, 1983; Galvez et al., 2007). Other investigations have suggested that calpains are activated during atrophy, and cleave myofibrillar proteins before their degradation by the ubiquitin proteasome system (Tidball and Spencer, 2002; Wei et al., 2005; Smith et al., 2008; McClung et al., 2009; Hudson et al., 2012). Here, we have uncovered a critical role for calpain-1 in the depolymerization and subsequent degradation of desmin filaments during atrophy induced by denervation or fasting. Their loss follows a specific sequence and involves an initial phosphorylation by GSK-3β and subsequent cleavage by calpain-1, which is a prerequisite for myofibril destruction and atrophy.

Results

Kinase-trap assay identifies GSK3-β as responsible for desmin filament phosphorylation during atrophy
To identify the critical kinase phosphorylating desmin filaments, we developed a mass spectrometry–based kinase-trap assay and studied mouse tibialis anterior (TA) muscles 3 d after denervation, when desmin phosphorylation increases (Volodin et al.,

2017). Homogenates from innervated and denervated muscles were incubated with a nonhydrolyzable ATP analogue, AMP-PNP, which is resistant to enzymes cleaving between β- and γ-phosphorus atoms. Because kinases catalyze protein phosphorylation by cleaving between these two atoms in ATP and transferring the γ-phosphoryl group of ATP to hydroxyl group on a substrate protein (Adams, 2001; Taylor and Kornev, 2011), in the presence of AMP-PNP, the kinases phosphorylating desmin filaments will bind desmin but fail to phosphorylate it, which should greatly facilitate their identification by mass spectrometry (Fig. 1 A). To isolate those kinases, we separated by centrifugation the insoluble pellets (containing desmin filaments and myofibrillar proteins) after incubation of muscle homogenates with AMP-PNP, and analyzed by mass spectrometry (Fig. 1 A and Table 1). Of 23 kinases that were identified, 14 were found to be at least threefold more abundant in the 3-d-denervated muscle than in the innervated control (Table 1). Among these kinases are ones that have been previously reported to phosphorylate desmin in vitro, including PKC, PKA, Ca^{2+}/calmodulin kinase II, and GSK3-β (Geisler and Weber, 1988; Inagaki et al., 1996; Huang et al., 2002; Agnetti et al., 2014), exemplifying the validity of our approach and the specificity of these physiological interactions. GSK3-β was deemed the most intriguing candidate as the kinase promoting desmin filament phosphorylation and loss during atrophy because it is the only kinase in our dataset that promotes protein phosphorylation that often leads to degradation (Quélo et al., 2004; Viatour et al., 2004; Gumbiner, 2005; Boucher et al., 2006). This kinase is primarily activated by the fall in PI3K-Akt signaling in many types of systemic atrophy, and also during the disuse atrophy induced by denervation as shown here (see below).

GSK3-β promotes atrophy by catalyzing desmin filament loss
To confirm biochemically that GSK3-β binds desmin filaments in denervated muscle, as suggested by our mass spectrometry analysis (Table 1), we analyzed soluble and insoluble fractions of muscle homogenates after incubation with AMP-PNP by SDS-PAGE and immunoblotting (Fig. 1 B). In innervated muscles, GSK3-β bound the insoluble pellet, but most of this enzyme was present in the soluble fraction (Fig. 1 B). However, 3 d after denervation, when phosphorylation of desmin filaments is rapid (Volodin et al., 2017), the association of GSK3-β with the insoluble pellet increased while its levels in the cytosol decreased (Fig. 1 B).

To determine whether desmin is a substrate for GSK3-β during atrophy in vivo, we suppressed GSK3-β function by the electroporation of a dominant negative GSK3-β (GSK-3-β-DN) into mouse TA, and induced atrophy by denervation or fasting. In parallel muscles, we down-regulated the ubiquitin ligase Trim32 by the transfection of specific shRNA (shTrim32) to cause accumulation of phosphorylated desmin filaments and compared them to GSK-3-β-DN–expressing muscles, where desmin filaments should accumulate in their nonphosphorylated form (Fig. 1, C and D). Desmin filaments were purified from transfected muscles by treating the insoluble pellet with 0.6 M KCl for 10 min to extract myofibrillar proteins (Cohen et al., 2012; Volodin et al., 2017). Immunoblotting with anti–phospho-serine showed increased phosphorylation of desmin filaments 3 d after denervation compared with control (Fig. 1 C), which was similar to the denervated

Aweida et al.
GSK3-β and calpain-1 promote desmin loss and atrophy

Journal of Cell Biology   3699
https://doi.org/10.1083/jcb.201802018

Figure 1. GSK3-β promotes atrophy by catalyzing desmin filament phosphorylation and loss. (A) A scheme for kinase-trap assay. **(B)** GSK3-β binds the myofibrillar pellet 3 d after denervation. Soluble and insoluble fractions from control and 3-d-denervated TA muscles were incubated with AMP-PNP and analyzed by SDS-PAGE and immunoblotting. **(C and D)** During atrophy, inhibition of GSK3-β markedly reduces desmin phosphorylation. Desmin filaments isolated from atrophying muscles expressing GSK3-β-DN, shTrim32, or shLacz were analyzed by immunoblotting. Right: Densitometric measurement of presented blots. $n = 3$. *, $P < 0.05$ vs. control; #, $P < 0.05$ vs. shLacz in atrophy; §, $P < 0.05$ vs. shTrim32 in atrophy. **(E)** GSK3-β phosphorylates desmin filaments in vitro. Pellets from denervated (3 d) muscles expressing GSK3-β-DN were subjected to in vitro phosphorylation reaction by recombinant GSK3-β. **(F)** Inhibition of GSK3-β with specific inhibitor prevents desmin phosphorylation and loss during fasting. TA muscles from fasted mice injected with GSK3-β inhibitor (L803mts) or vehicle were analyzed by immunoblotting. Right: Densitometric measurement of presented blots. $n = 3$ for DMSO. $n = 4$ for GSK3-β inhibitor. *, $P < 0.05$. **(G)** During fasting, GSK3-β inhibition with a dominant negative prevents myofibril destruction. Equal fractions (0.1%) of myofibrils from GSK3-β-DN– or shLacz-expressing muscles from fed or fasted mice were analyzed by SDS-PAGE and Coomassie blue staining. **(H)** GSK3-β inhibition markedly reduces fiber atrophy during fasting. Measurements of cross-sectional areas of 500 fibers expressing GSK3-β (black bars) versus 500 nontransfected fibers (open bars) in the same muscle. $n = 5$ mice. **(I)** Inhibition of GSK3-β blocks the loss of muscle mass during fasting. Mean weights of electroporated muscles are plotted as percentage of fed control. $n = 3$. *, $P < 0.05$ vs. shLacz in atrophy.

Table 1. Kinases that bound the insoluble fraction of 3-d-denervated mouse TA muscle

Name	Gene	No. of peptides	No. of unique peptides	Fold change (denervated/innervated)
Cyclin dependent kinase 5	CDK5	52	1	Not found in innervated
Src family tyrosine kinase	LYN	51	1	4.56
Mitogen-activated protein kinase 12	MAPK12	10	11	3.75
Protein kinase C θ	PRKCQ	7	9	3.15
cAMP-dependent protein kinase type II-α regulatory subunit	PRKAR2A	6	17	Not found in innervated
Calcium/calmodulin-dependent protein kinase type II subunit α	CAMK2A	6	3	4.73
MAP kinase-activated protein kinase 2	MAPKAPK2	6	5	Not found in innervated
Pyruvate dehydrogenase (acetyl-transferring) kinase	PDK4	5	7	6.27
Glycogen synthase kinase-3 β	GSK3B	4	2	Not found in innervated
Integrin-linked protein kinase	ILK	3	12	Not found in innervated
N-acetylgalactosamine kinase	GALK2	3	4	Not found in innervated
Casein kinase II	CSNK2A	1	3	3.4
Dephospho-CoA kinase domain-containing protein	DCAKD	2	4	4.84
Serine/threonine-protein kinase RIO3	RIOK3	1	2	Not found in innervated

Protein kinases were purified together with the insoluble fraction of TA muscle 3 d after denervation using a kinase-trap assay and identified by mass spectrometry.

muscles expressing shTrim32. At this time desmin filaments are intact, even though their phosphorylation increased (Fig. 1 C; Volodin et al., 2017). However, inhibition of GSK3-β by the electroporation of GSK3-β-DN blocked this increase in phosphorylation, indicating that after denervation, this kinase is responsible for desmin filament phosphorylation.

To learn whether GSK3-β serves a similar role in other types of atrophy, we inhibited this kinase in mouse muscles during fasting and analyzed the effects on desmin filament phosphorylation. Phosphorylated desmin filaments were reduced during fasting compared with fed control, but not when Trim32 was down-regulated with shRNA (Fig. 1 D); instead, desmin accumulated as insoluble phosphorylated filaments (Fig. 1 D). Strikingly, inhibition of GSK3-β with GSK3-β-DN also blocked this loss of desmin filaments upon fasting, but desmin filaments accumulated as nonphosphorylated species (Fig. 1 D). It is noteworthy that in normal muscles expressing GSK3-β-DN for 4 d, desmin filament phosphorylation did not decrease (Fig. S1 A).

To determine if desmin is a direct substrate for GSK3-β, we purified desmin filaments from 3-d-denervated muscles expressing GSK3-β-DN and assayed their susceptibility to phosphorylation by recombinant GSK3-β (Fig. 1 E). Purified GSK3-β phosphorylated desmin filaments in vitro but not when the divalent cation chelating agent, EGTA, was added (Fig. 1 E, lanes 2 and 4). Under the same conditions, a nonrelevant kinase, GCN2, failed to phosphorylate desmin filaments (Fig. S2). Consistently, inhibition of GSK3-β by the injection of mice with a GSK3-β specific inhibitor (L803-mts; Plotkin et al., 2003) blocked desmin loss upon fasting, and desmin accumulated in the soluble fraction and as insoluble nonphosphorylated filaments (Fig. 1 F). Thus,

during atrophy induced by denervation or fasting, GSK3-β is the primary kinase phosphorylating desmin filaments.

Reducing GSK3-β function during atrophy blocked desmin phosphorylation and depolymerization, which should attenuate myofibril loss and fiber atrophy (Cohen et al., 2012; Volodin et al., 2017). Consistently, analysis of isolated myofibrils by SDS-PAGE and Coomassie staining indicated that during fasting their content decreased below levels in control muscles from fed animals, but not when GSK3-β was inhibited with GSK3-β-DN (Fig. 1 G). Furthermore, the mean cross-sectional area of 500 fibers expressing GSK3-β-DN was much greater than that of 500 adjacent nontransfected fibers in the same atrophying muscle (Fig. 1 H), indicating that in fibers where GSK3-β was inhibited atrophy was attenuated. Finally, the reduction in mean TA weights caused by fasting (by 22%) was completely blocked in muscles electroporated with GSK3-β-DN (Fig. 1 I). These effects were specific to atrophy because inhibition of GSK3-β in normal muscle for 4 d had no effect on myofibril content or muscle weight (Fig. S1, B and C). Thus, GSK3-β catalyzes desmin filament phosphorylation and depolymerization, which triggers myofibril destruction and atrophy.

GSK3-β is activated at an early phase during atrophy when PI3K–Akt–FoxO signaling is low

We next determined the time course of GSK3-β activation at different times after denervation. Analysis of the soluble fraction of denervated muscles showed that by 3 d after denervation, protein levels as well as phosphorylation of PI3K, Akt, FoxO3, and GSK3-β were lower than in innervated control muscles (Fig. 2 A), as has also been demonstrated previously (Tang et al.,

2014). These findings indicate decreased PI3K-Akt signaling and activation of GSK3-β when phosphorylation of desmin filaments is rapid (Fig. 1 C). The reduction in the total amount of GSK3-β in the soluble fraction of 3-d-denervated muscles is consistent with the increased association of this kinase with desmin filaments (Fig. 1 B). Interestingly, the levels of phosphorylated PI3K, Akt, FoxO3, and GSK3-β increased at 7 d after denervation and remained high for at least seven more days (Fig. 2 A), which correlates with the time course of sensitivity to insulin by denervated muscle (Davis and Karl, 1988). This increased PI3K-Akt activity, and the resulting inhibition of GSK3-β, is consistent with this kinase playing a role in desmin phosphorylation early after denervation.

Surprisingly, GSK3-β seemed to contribute to this fall in PI3K-Akt activity at 3d after denervation, because GSK3-β inhibition with GSK3-β-DN enhanced PI3K-Akt signaling, inhibited FoxO, and reduced the expression of the atrophy-related gene Atrogin1 (Fig. 2, B and D). MuRF1 seemed to show a similar reduction in expression in the GSK3-β-DN–transfected denervated muscles, but this trend did not reach statistical significance (P = 0.05). A similar role for GSK3-β in the inhibition of PI3K-Akt signaling has been previously demonstrated in cultured Th17 cells (Gulen et al., 2012). To further clarify this role of GSK3-β, we studied the rapid atrophy induced by fasting. Normally, during fasting, FoxO is activated (dephosphorylated) by the fall in insulin-PI3K-Akt signaling, and stimulates atrogenes expression (Fig. 2, C and D). However, GSK3-β inhibition by GSK3-β-DN resulted in a marked increase in FoxO phosphorylation and decreased MuRF1 and atrogin-1 expression during fasting (Fig. 2, C and D). Consistently, previous studies demonstrated a role for GSK3-β in promoting atrophy via the induction of atrogenes (Verhees et al., 2011). Interestingly, GSK3-β inhibition did not cause an increase in Akt phosphorylation, suggesting that during fasting, GSK3-β stimulates FoxO transcriptional activity by other mechanisms (not through inhibition of Akt activity), as proposed before (Huo et al., 2014). Although inhibition of GSK3-β in normal muscle for 4 d caused an increase in Akt phosphorylation, it had no effect on FoxO activity, atrogene expression, or rates of protein synthesis (Fig. S1, D–F). Thus, GSK3-β triggers the FoxO-mediated expression of the atrogene program, partly by eliciting a reduction in PI3K-Akt-FoxO signaling at an early phase in various types of atrophy.

In addition to regulating protein degradation, GSK3-β limits cell size also by reducing rates of protein synthesis (Rommel et al., 2001; Hardt et al., 2004). During fasting, GSK3-β inhibition in TA muscles enhanced protein synthesis because puromycin incorporation into newly translated proteins was higher than in shLacz-expressing muscles (Fig. 2 E). In contrast, GSK3-β inhibition had no effect on protein synthesis rates in 3-d-denervated muscle (Fig. S3). Thus, the inhibition of atrogene expression during fasting together with the maintenance of normal PI3K–Akt-mTOR signaling and enhanced protein synthesis can account for the dramatic blockage of muscle wasting observed above (Fig. 1, G–I). The accumulation of desmin filaments and myofibrillar proteins by GSK3-β inhibition during atrophy resulted primarily from reduced degradation (rather than

increased synthesis) because under these conditions desmin and myofibrillar actin were not induced (Fig. S4).

Calpain-1 down-regulation attenuates atrophy upon denervation or fasting

Although phosphorylation of desmin filaments by GSK3-β and subsequent ubiquitination increased rapidly at 3 d after denervation, this cytoskeletal network slowly depolymerized, and loss of phosphorylated desmin filaments was evident only between 7 and 10 d after nerve sectioning (Volodin et al., 2017). Thus, the loss of desmin filaments during atrophy appears to require an additional signal, presumably a proteolytic cleavage that will enhance their dissociation. We searched our mass spectrometry data (Fig. 1) for enzymes that promote proteolysis and bound the phosphorylated insoluble pellet, and found three members of the Ca^{2+}-dependent cysteine proteases, calpain-1 catalytic and small subunits, calpain-2 and calpain-3 (Table 2). Because calpain-1 is activated in various types of atrophy (McClung et al., 2009; Macqueen et al., 2010), binds the Z-bands where desmin filaments are aligned (Goll et al., 1991; Raynaud et al., 2005), and promotes proteolysis in skeletal and cardiac muscle (Geesink et al., 2006; Galvez et al., 2007; Kemp et al., 2013) and desmin loss in ischemic heart (Blunt et al., 2007), we hypothesized that this enzyme also catalyzes the depolymerization of phosphorylated desmin filaments during atrophy. To test this idea, we first determined the time course of calpain activation in muscles atrophying because of food deprivation or denervation using the calpain-specific fluorogenic substrate N-succinyl-Leu-Tyr-7-amido-4-methylcoumarin (SLY-AMC; Fig. 3, A–C). Samples not containing CaCl$_2$ were used to verify a specific SLY-AMC cleavage by cellular calpains. Analysis of equal amounts of insoluble filaments from control and atrophying muscles showed that calpain activity increased already by the first day of food deprivation (Fig. 3 A). 14 d after denervation, there was no increase in calpain activity (Fig. 3 B) but rather at an earlier phase after denervation (7 d; Fig. 3 C), just when depolymerization of desmin filaments is accelerated (Volodin et al., 2017).

Calpains bound the insoluble pellet containing desmin already at 3 d after denervation (Table 2) but their activity increased only 4 d later (Fig. 3 C). This delayed response to muscle denervation may result from changes in free cellular Ca^{2+} levels, which are required for calpain activation. To test this idea, we modified a previously published protocol (Sato et al., 1988) to measure intracellular Ca^{2+} levels in mouse muscles using the fluorescent indicator calcium green-1-AM. Once metabolized by cellular esterases, this indicator binds free Ca^{2+} and generates a fluorescence signal. Thin strips of control and atrophying muscles were incubated in vitro in the presence or absence of calcium green-1-AM, washed, and then excited at 488 nm. Fluorescent imaging of these muscles clearly showed increased cellular Ca^{2+} levels during fasting compared with fed controls (Fig. 3 D). Furthermore, the fluorescent signal was low in innervated and 3-d-denervated muscles (Fig. 3 E), but peaked at 7 d after denervation, as reported (Cea et al., 2013), just when calpain activity is maximal (Fig. 3 C) and desmin depolymerizes.
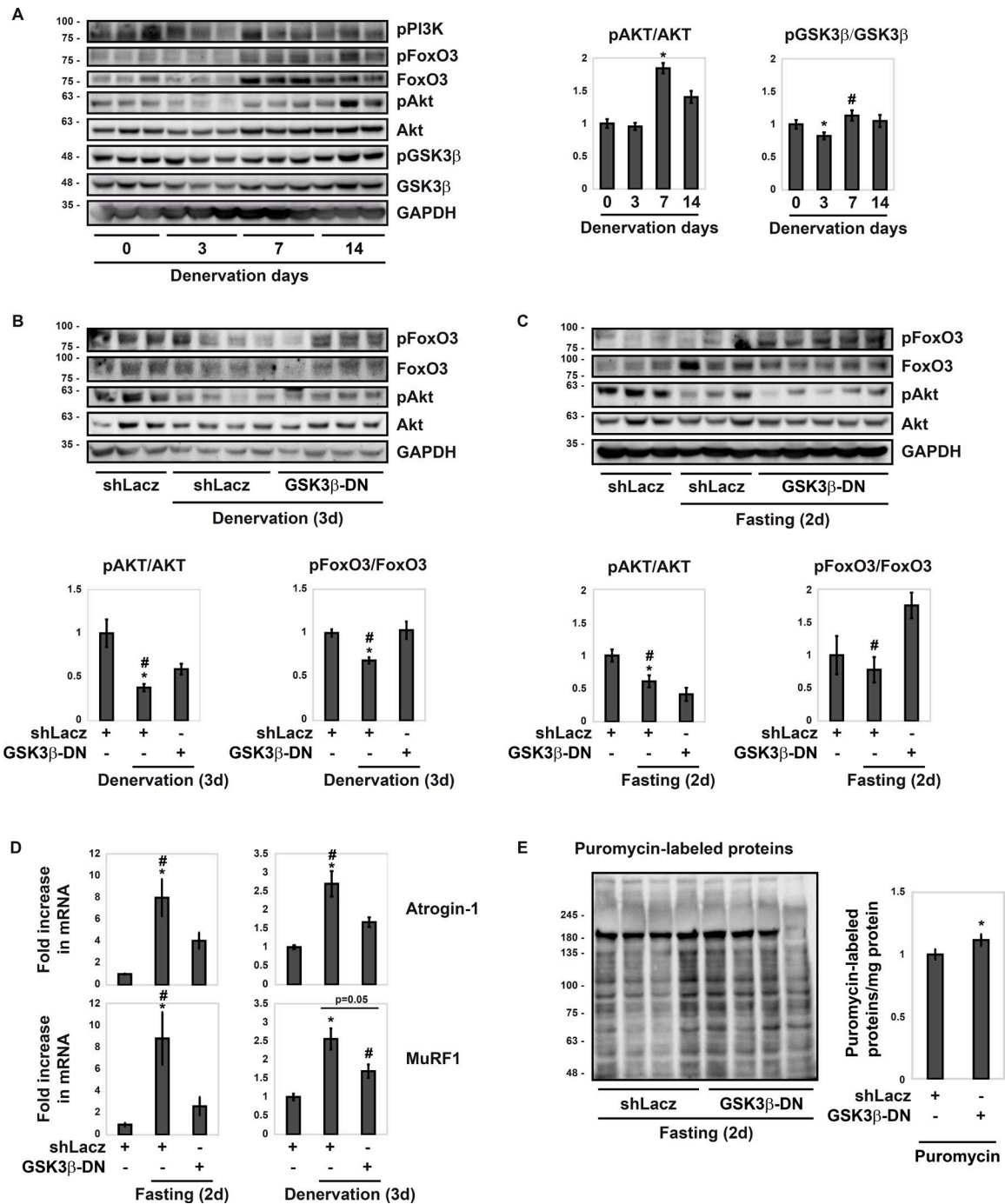
Figure 2. **GSK3-β is activated at an early phase during atrophy when PI3K–Akt–FoxO signaling is low. (A)** Time course of PI3K-Akt activation after muscle denervation. Right: Densitometric measurement of presented blots. *n* = 3. *, P < 0.05 vs. innervated; #, P < 0.05 vs. 3-d-denervated muscles. **(B and C)** Inhibition of GSK3-β with GSK3-β-DN activates FoxO3 on denervation (B) or fasting (C). Transfected muscles were analyzed by immunoblotting. Bottom: Densitometric measurement of presented blots. *n* = 3 for shLacz. *n* = 4 for GSK3-β-DN. *, P < 0.05 vs. control; #, P < 0.05 vs. GSK3-β-DN. **(D)** GSK3-β inhibition reduces MuRF1 and Atrogin1 expression during atrophy. RT-PCR of mRNA preparations from atrophying and control muscles expressing shLacz or GSK3-β-DN using primers for MuRF1 and Atrogin1. Data are plotted as the mean fold change relative to control ± SEM. *n* = 5. *, P < 0.05 vs. control. #, P < 0.05 vs. GSK3-β-DN. **(E)** During fasting, inhibition of GSK3-β increases rates of protein synthesis. Mice were injected with puromycin, and soluble fractions of electroporated muscles were analyzed by immunoblotting. Right: Densitometric measurement of the presented blot. *n* = 4. *, P < 0.05 vs. shLacz.

Calpain-1 is necessary for the loss of phosphorylated desmin filaments and atrophy

To test whether calpain-1 is essential for desmin loss and atrophy, we suppressed its expression with a specific shRNA (shCAPN1), which efficiently reduced calpain-1 protein levels (but not the levels of its related family member calpain-2) in the cytosol below levels in denervated and innervated muscles (Fig. 4 A). In these muscles, fiber atrophy was markedly attenuated on denervation (14 d) or fasting (2 d) because the cross-sectional area of nontransfected atrophying fibers was smaller than those fibers

Table 2. Calpains bind the insoluble fraction of 3-d-denervated TA mouse muscle

Name	Gene	No. of unique peptides
Calpain 1 catalytic subunit	CAPN1	24
Calpain small subunit 1	CAPNS1	3
Calpain 2	CAPN2	18
Calpain 3	CAPN3	7

Calpains were purified together with the insoluble fraction of TA muscle 3 d after denervation and identified by mass spectrometry.

expressing shCAPN1 (Fig. 4, B and C). A reduction in fiber atrophy upon shCAPN1 expression has been also observed at 7 d after denervation (Fig. 4 D), when Ca^{2+} levels rise (Fig. 3 E) and calpain activity is maximal (Fig. 3 C). This reduction in fiber atrophy during fasting or at 14 d after denervation resulted largely from inhibition of myofibril destruction, whose content in the atrophying muscles expressing shCAPN1 no longer differed significantly from that in control muscles (Fig. 4, E and F).

To determine if desmin is a direct substrate for calpain-1, we isolated desmin filaments from normal TA and analyzed their cleavage by recombinant calpain-1. Increasing concentrations of calpain-1 facilitated cleavage of desmin filaments, as demonstrated by the reduction in full-length desmin and the appearance of desmin fragments (Fig. 5 A). Desmin fragments also accumulate in atrophying muscle in vivo and are probably formed by the incomplete degradation of desmin monomers by calpain-1, other proteases (e.g., caspases), or the proteasome (Chen et al., 2003; Cohen et al., 2012).

To learn whether desmin filaments are substrates for calpain-1 in vivo, we analyzed the effects of calpain-1 down-regulation on
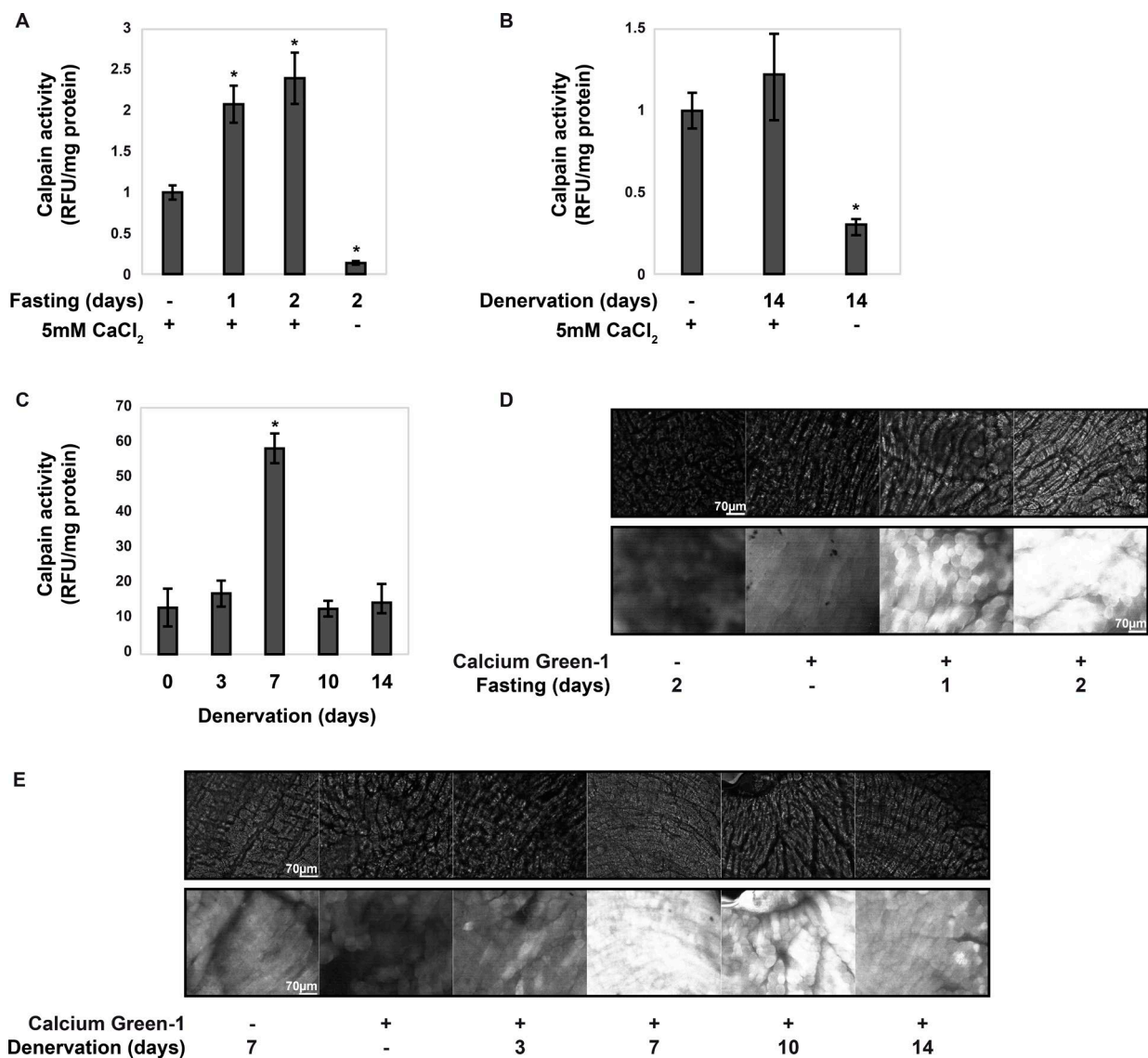

Figure 3. **During atrophy, calpain activity increases when cellular Ca^{2+} levels rise. (A–C)** Calpain activity was measured in the insoluble fraction of normal and atrophying muscles during fasting (A) or after denervation (B and C) using the fluorogenic substrate SLY-AMC. n = 3. *, P < 0.05 vs. control. **(D and E)** Cellular Ca^{2+} levels were measured in strips of control and atrophying muscles using calcium green-1-AM. n = 3. Top, transmitted light; bottom, fluorescence (480 nm). Scale bar: 70 µm.
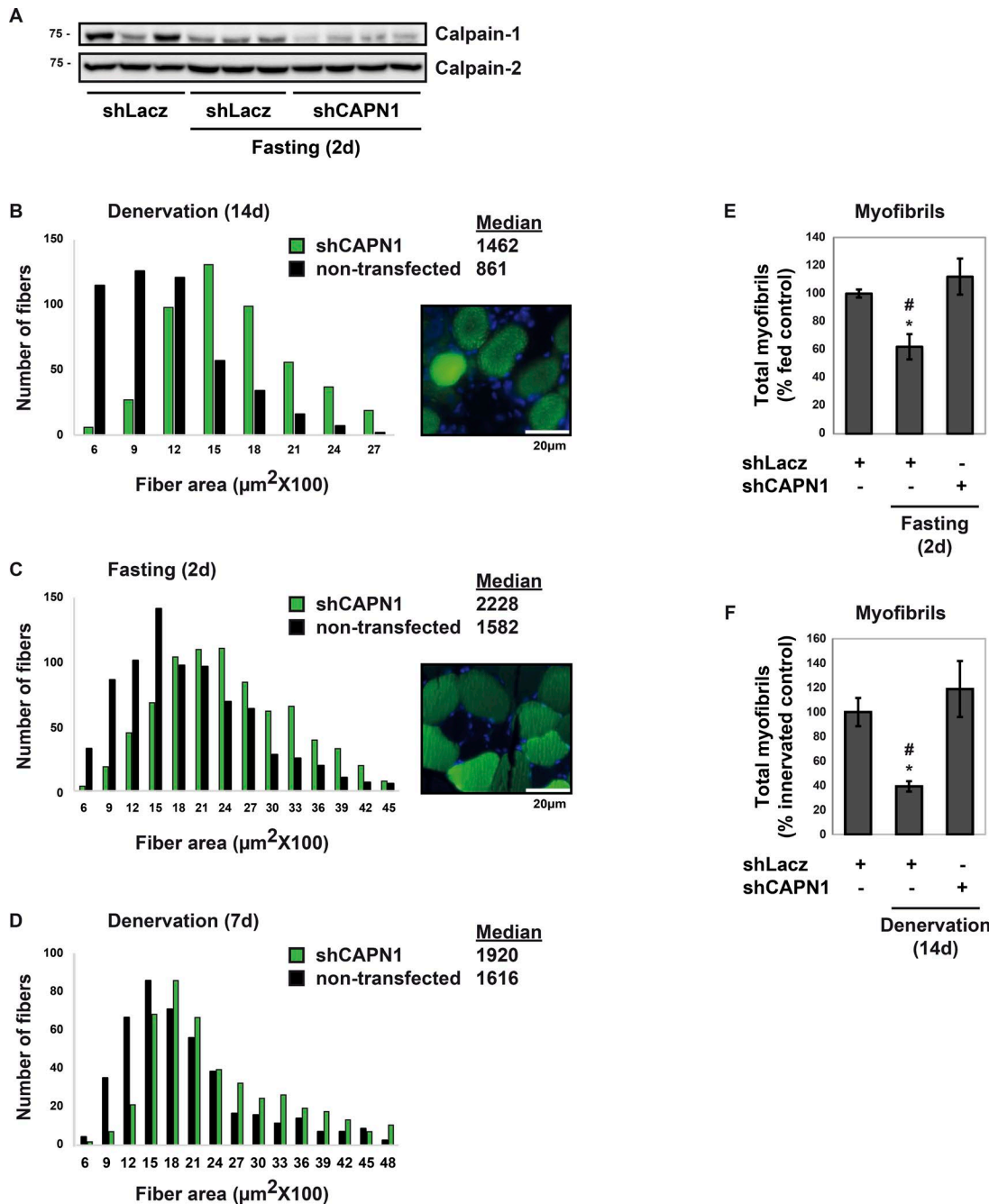
Figure 4. **Calpain-1 down-regulation blocks myofibril loss and atrophy.** TA muscles were electroporated with shCAPN1 or shLacz, and atrophy was induced by fasting (2 d) or denervation (7 or 14 d). **(A)** shRNA-mediated knockdown of calpain-1 in TA muscles from fasted mice. Soluble extracts were analyzed by immunoblotting. **(B–D)** Calpain-1 down-regulation reduces atrophy upon denervation (B and D) or fasting (C). Measurements of cross-sectional areas of 500 fibers transfected with shCAPN1 (and expressing GFP, green bars) versus 500 nontransfected fibers (black bars) in the same muscle. $n = 3$ mice. Scale bar: 20 μm. **(E and F)** Calpain-1 down-regulation blocks myofibril loss upon fasting (E) or denervation (F). The mean content of myofibrils per electroporated muscle is presented as percentage of control. $n = 4$. *, $P < 0.05$ vs. control; #, $P < 0.05$ vs. shCAPN1.

the content of desmin filaments during atrophy. At 7 d after denervation, before any significant loss of desmin can be observed (Volodin et al., 2017), phosphorylated desmin filaments accumulated similarly in shLacz or shCAPN1 expressing muscles (Fig. 5 B). However, in the muscles denervated for 14 d, the content of phosphorylated desmin filaments decreased below levels in contralateral innervated limbs, but not when calpain-1 was down-regulated with shRNA (Fig. 5 C). Calpain-1 down-regulation also completely

blocked the loss of phosphorylated desmin filaments during fasting (Fig. 5 D). Thus, calpain-1 is essential for loss of desmin filaments, the resulting myofibril destruction, and atrophy.

During atrophy, phosphorylation by GSK3-β is essential for desmin filament depolymerization by calpain-1
These observations make it likely that phosphorylation of desmin filaments by GSK3-β during atrophy increases their
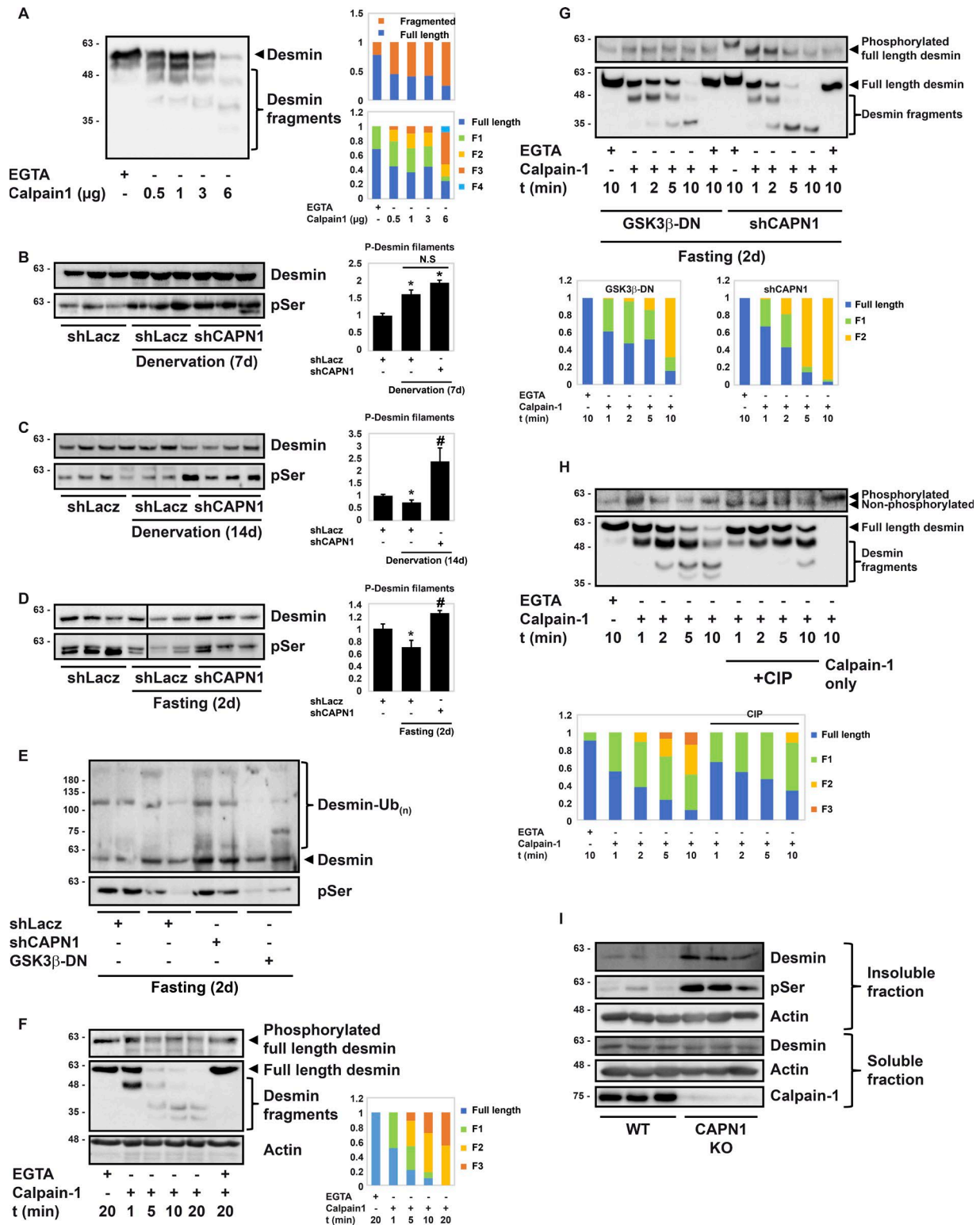
Figure 5. **Desmin filament phosphorylation is essential for depolymerization by calpain-1. (A)** Desmin is a direct substrate of calpain-1. In vitro cleavage of desmin filaments by recombinant calpain-1. Right: Densitometric measurement of presented blots. Full-length desmin and desmin fragments (F) are depicted as a fraction of the total amount of desmin. **(B)** Down-regulation of calpain-1 7 d after denervation does not affect desmin integrity. Desmin filaments were analyzed by immunoblotting. Right: Densitometric measurement of presented blots. n = 3. *, P < 0.05 vs. innervated control. **(C and D)** Down-regulation of calpain-1 prevents loss of phosphorylated desmin upon denervation (C) or fasting (D). Desmin filaments were analyzed by immunoblotting. Right: Densitometric measurement of presented blots. n = 3. *, P < 0.05 vs. control; #, P < 0.05 vs. shLacz in atrophy. Black line indicates the removal of an intervening lane for presentation purposes. **(E)** GSK3-β–mediated desmin filament phosphorylation precedes depolymerization by calpain-1. Insoluble fractions of muscles expressing shCAPN1, GSK3-β-DN, or shLacz were analyzed by immunoblotting. **(F–H)** Insoluble fractions from transfected muscles were incubated with purified calpain-1 for the indicated times. Protein cleavage was detected by immunoblotting. In densitometric measurement of presented blots, full-length desmin

susceptibility to cleavage by calpain-1. To determine if calpain-1 functions after GSK3-β in the turnover of desmin filaments, we compared the effects of calpain-1 down-regulation (with shCAPN1) and GSK3-β inhibition (with GSK3-β-DN) on the total amount of phosphorylated desmin filaments during fasting. As shown (Fig. 5 D; Cohen et al., 2012), phosphorylated desmin filaments were lost during fasting (Fig. 5 E), but not when calpain-1 was down-regulated; instead, desmin accumulated as insoluble phosphorylated and ubiquitinated species (Fig. 5 E, lanes 5 and 6). However, inhibition of GSK3-β with GSK3-β-DN prevented phosphorylation, ubiquitination, and depolymerization of desmin filaments, which now accumulated as nonphosphorylated and nonubiquitinated species (Fig. 5 E, lanes 7 and 8). Thus, during atrophy, phosphorylation of desmin filaments by GSK3-β precedes their ubiquitination (e.g., by Trim32) and depolymerization by calpain-1.

To investigate whether phosphorylation by GSK3-β is required for cleavage by calpain-1, we first determined if calpain-1 preferentially catalyzes the loss of phosphorylated desmin filaments during atrophy. For this purpose, we isolated the insoluble pellet from muscles lacking calpain-1 from fasted mice, and measured cleavage of desmin and myofibrillar actin over time by recombinant calpain-1 (Fig. 5 F). Calpain-1 efficiently and preferentially cleaved desmin filaments, but not myofibrillar actin, which remained intact in these samples (Fig. 5 F). Furthermore, desmin filaments in atrophying muscles expressing shCAPN1, which contained more phosphorylated species than in GSK3-β-DN–expressing muscles, were cleaved more efficiently by recombinant calpain-1 as indicated by the faster turnover of full-length desmin and rate of appearance of desmin fragments (Fig. 5 G). Finally, desmin filaments isolated from atrophying muscles expressing shCAPN1 and pretreated with the alkaline protein phosphatase calf intestinal (CIP) were significantly less sensitive for cleavage by calpain-1 (Fig. 5 H), indicating that phosphorylation of desmin filaments enhances their recognition and cleavage by this protease. Thus, during atrophy, phosphorylation of desmin filaments facilitates their depolymerization by calpain-1.

Interestingly, calpain-1 is also required for normal turnover of desmin filaments, because in muscles from calpain-1 null mice (Seinfeld et al., 2016) desmin accumulated as insoluble phosphorylated filaments (Fig. 5 I). Despite these changes, the total amount of myofibrillar actin, which is stabilized by desmin at the Z-bands (Conover et al., 2009), was similar in muscles from calpain-1 null and WT mice, indicating that the rapid loss of myofibrillar actin during atrophy requires an additional signal beyond desmin disassembly, presumably the atrophy-induced loss of myofibril stabilizing components (Cohen et al., 2009) and induction of p97/VCP (Volodin et al., 2017).

Discussion

We have uncovered the mechanism promoting desmin filament disassembly, which causes myofibril destruction during atrophy, and involves the protein kinase GSK3-β and the Ca²⁺-specific protease calpain-1 (Fig. 6). As shown here, on denervation or fasting, solubilization of the desmin cytoskeleton follows a specific sequence involving phosphorylation by GSK3-β, ubiquitination, and calpain-1–dependent depolymerization (Fig. 6). Previously, we and others demonstrated that this ubiquitination is dependent on the ubiquitin ligase Trim32 (Cohen et al., 2012; Volodin et al., 2017). Thus, these studies together with the prior ones emphasize a common mechanism that stimulates proteolysis via the proteasome during atrophy throughout an ordered and tightly regulated process.

The role of desmin filaments in tissue architecture has been extensively studied (Lazarides and Hubbard, 1976; Lazarides, 1978; Milner et al., 1996), but the fate of this cytoskeletal network during atrophy and the influence of its depolymerization on protein degradation have been generally overlooked. We and others previously showed that during atrophy induced by denervation or fasting, disassembly and loss of phosphorylated desmin filaments triggers myofibril destruction (Cohen et al., 2012; Volodin et al., 2017), and the present studies demonstrate that GSK3-β and calpain-1 are critical in promoting this loss. Reducing GSK3-β function by either a dominant-negative or a specific inhibitor prevented desmin phosphorylation, ubiquitination, and depolymerization, and markedly reduced myofibril loss and atrophy (Figs. 1 and 5 E). Similarly, down-regulation of calpain-1 blocked desmin loss, myofibril breakdown, and atrophy (Figs. 4 and 5), and caused accumulation of phosphorylated desmin filaments as ubiquitinated species (Fig. 5 E). Because calpain-1 does not harbor a bona fide ubiquitin binding domain, the ubiquitination of desmin filaments (perhaps within the rod domain as suggested; Ye et al., 2014) probably triggers conformational changes that expose calpain-1 cleavage sites on desmin and facilitate depolymerization. A similar role for ubiquitination in promoting cleavage by calpains has been proposed (Sagar et al., 2007; Watkins et al., 2012). This cleavage by calpain-1 probably releases ubiquitinated desmin from the insoluble filaments to the cytosol, where it is presumably more susceptible to the proteasome. Alternatively, solubilization of ubiquitinated desmin filaments may require additional factors such as the p97–VCP ATPase complex (Rabinovich et al., 2002; Volodin et al., 2017), which extracts ubiquitinated proteins from larger structures (e.g., the ER membrane in the ERAD pathway) before proteasomal degradation.

These studies demonstrate that phosphorylated desmin filaments, which accumulated in atrophying muscles expressing shCAPN1, were cleaved more rapidly by recombinant calpain-1 than those filaments isolated from GSK3-β-DN–expressing

and desmin fragments (F) are depicted as a fraction of the total amount of desmin. **(F)** Desmin filaments from muscles expressing shCAPN1 from fasted mice are selectively cleaved by calpain-1. **(G)** Phosphorylation of desmin filaments facilitates cleavage by calpain-1. Cleavage of desmin filaments from atrophying muscles expressing GSK3-β-DN or shCAPN1 was analyzed in parallel. **(H)** Desmin filaments from muscles expressing shCAPN1 during fasting were treated with CIP (lanes 6–10) or left untreated (lanes 1–5) and then subjected to cleavage by recombinant calpain-1. **(I)** In muscles from calpain-1 null mice, desmin filaments accumulate. Insoluble and soluble fractions of muscles from WT and calpain-1 knockout mice were analyzed by immunoblotting.
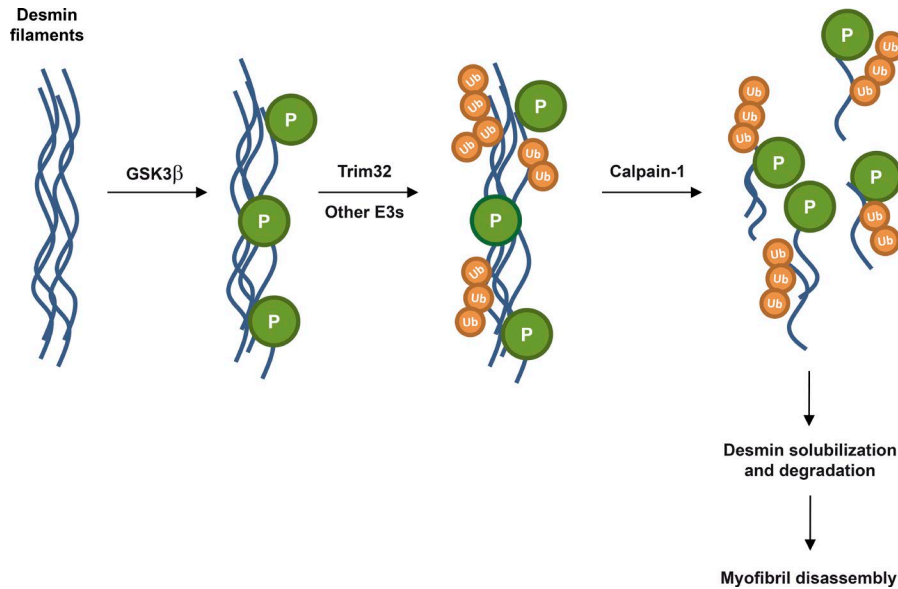
Figure 6. **Proposed mechanism for desmin filament loss during atrophy.** Phosphorylation of desmin filaments by GSK3-β precedes and promotes ubiquitination by Trim32 and depolymerization by calpain-1, ultimately leading to myofibril loss and atrophy. Thus, phosphorylation by GSK3-β is a critical early step for desmin filament destruction and overall protein degradation during atrophy. Consequently, GSK3-β and calpain-1 may represent new therapeutic targets to reduce myofibril breakdown and muscle wasting during aging or disease.

muscles, where desmin accumulated as nonphosphorylated filaments (Fig. 5 G). This cleavage of desmin filaments was selective, because myofibrillar actin in those fractions remained intact (Fig. 5 F; Goll et al., 1991). Thus, the increased phosphorylation of desmin filaments during atrophy enhances their differential disassembly by calpain-1. In fact, the strongest evidence for the importance of desmin phosphorylation was our finding that phosphatase treatment markedly reduced desmin cleavage by purified calpain-1 (Fig. 5 H). Consistently, previous studies demonstrated that calpain-1 acts preferentially on phosphorylated substrates to promote their degradation (Shen et al., 2001). Clearly, phosphorylation of desmin filaments enhances their recognition by this enzyme during atrophy. However, substrate phosphorylation cannot be a prerequisite for cleavage by calpain-1 because in some cases phosphorylation rather protects from cleavage by this enzyme (Raynaud et al., 2006). Phosphorylation of desmin filaments by GSK3-β is also required for ubiquitination by Trim32 (Cohen et al., 2012; Volodin et al., 2017), which we show here precedes disassembly by calpain-1.

As shown here, activation of GSK3-β is a critical early step for desmin filament destruction, and as suggested before (Evenson et al., 2005; Verhees et al., 2011), for overall protein degradation during atrophy. GSK3-β activity is inhibited primarily through phosphorylation by the insulin-PI3K-Akt pathway (Cross et al., 1995) and is activated in atrophy during fasting and in many systemic human diseases by inhibition of this pathway. Here, we demonstrate that several days after denervation, GSK3-β renders its own activation by eliciting a negative feedback loop on PI3K-Akt-FoxO pathway (Fig. 2, B and C). This fall in insulin signaling correlates with the reduced insulin sensitivity and glucose metabolism 3 d after denervation (Davis and Karl, 1988). GSK3-β may also be activated by changes in cellular localization, phosphorylation on Tyr216, or phosphorylation of its substrates (Meijer et al., 2004). Furthermore, previous studies have indicated that GSK3-β acts on its substrates only after they have been phosphorylated by another kinase. Consistently, the inhibition of this enzyme during atrophy resulted in the accumulation of desmin filaments that

were phosphorylated to some extent (Fig. 1, C and D). The priming phosphorylation of GSK3-β substrates is required to generate a GSK3-β consensus sequence $SX_{3or4}S$, with the carboxy-terminal serine phosphorylated (Cole and Sutherland, 2008). Interestingly, desmin head domain harbors a potential GSK3-β consensus sequence, $S_{28}PLSS_{32}$, where phosphorylation of desmin filaments (on serines 28, 32, and 68) occurs during fasting (Cohen et al., 2012). Several kinases that may catalyze the priming phosphorylation of GSK3-β's substrates, including PKC, CDK5, PKA, and CK2 (Meijer et al., 2004), were identified by our kinase-trap assay bound to the insoluble pellet of denervated muscle, together with GSK3-β (Table 1). It is unclear if any of these kinases is activated in muscle during atrophy and phosphorylates desmin filaments or the myofibrils. Among these enzymes, PKC is most likely to serve as the priming kinase because desmin phosphorylation by PKC is linked to disarray of myofibrils in cardiomyocytes (Huang et al., 2002), and activation of PKC in muscle induces proteolysis (Wyke and Tisdale, 2006). In any case, GSK3-β clearly plays a primary and critical role in the overall proteolysis during atrophy because its inhibition is sufficient to prevent desmin loss, myofibril breakdown, and atrophy (Fig. 1). In addition to this role in promoting protein breakdown, GSK3-β seems to inhibit protein synthesis during fasting (Fig. 2 E), but not after denervation (Fig. S3), perhaps by reducing the function of the translation initiation factor eIF2B (Hardt et al., 2004). However, the beneficial effects of GSK3-β inhibition on desmin filaments, myofibrillar proteins, and atrophy during fasting seem to result primarily from reduced protein degradation, because under these conditions desmin and myofibrillar actin were not induced (Fig. S4).

After denervation, phosphorylation of desmin filaments by GSK3-β increased rapidly (Fig. 1 C), but the depolymerization of this cytoskeletal network occurred only 4–7 d later (Volodin et al., 2017). As shown here, this dissociation of desmin filaments requires calpain-1, which seems to be activated only 7 d after denervation when cytosolic Ca^{2+} levels rise (Fig. 3, C–E), and just before significant loss of desmin filaments or myofibrils can be seen (Volodin et al., 2017). In denervated muscle, Ca^{2+} is less

efficiently pumped out of the cytosol (Finol et al., 1981; Zorzato et al., 1989; Cea et al., 2013), and the resulting rise in intracellular Ca^{2+} concentration activates Ca^{2+}-dependent enzymes including calpains. 7 d after denervation, the increase in calpain activity probably reflects calpain-1 function because reducing its expression with shCAPN1 was sufficient to block atrophy (Fig. 4). At this time, desmin filaments and myofibrils are intact, and calpain-1 promotes fiber atrophy (Fig. 4 D) most likely by catalyzing the loss of cytosolic proteins. However, the accumulative beneficial effects of calpain-1 down-regulation on overall proteolysis and atrophy can be observed clearly only at a later phase (at 14 d), when both the initial loss of desmin filaments and the resulting myofibril destruction are blocked (Figs. 4 F and 5 C). The gradual reduction in muscle mass observed before this time point (7 d) may result from degradation of soluble proteins and organelles (e.g., mitochondria), degradation of "easily releasable" myofibrils—a small fraction of myofibrillar proteins that are easily released upon homogenization and seem to comprise the outer layers of the myofibrils (Etlinger et al., 1975), and slow degradation of small regulatory proteins that stabilize the myofibril, which are lost sooner than myofibrillar myosin and actin, and by rigorous analysis a reduction in their content is evident only at 10 d (Cohen et al., 2009). Early changes in protein synthesis rates (Goldspink, 1976; Davis and Karl, 1988), for example by the fall in PI3K-Akt signaling 3 d after denervation (Fig. 2, A and B), may also contribute to the slow and gradual reduction in protein content at this time point, until desmin and myofibril breakdown is accelerated at a later phase. Possibly, this gradual reduction in protein content occurs until sufficient amount of desmin is phosphorylated and degraded, and facilitates the subsequent myofibril destruction. In fact, we recently showed that there are early and late phases during the atrophy process involving an initial loss of desmin filaments and a later loss of myofibrils, which also requires the induction of genes that promote proteolysis by PAX4 (Volodin et al., 2017). Thus, our findings argue strongly that desmin depolymerization is an early critical step for overall protein degradation during atrophy.

It remains to be determined if by promoting the loss of desmin filaments, calpain-1 also compromises the integrity of Z-bands, which should loosen the highly ordered structure of the thin filaments and the associated thick filaments (Cohen et al., 2009). Consistently, previous studies in vitro indicated that the principal component of Z-bands, α-actinin, can be released from purified myofibrils by calpain-1 or by increasing Ca^{2+} concentration (Condeelis and Vahey, 1982; Goll et al., 1991). In knockout mice lacking calpain-1, phosphorylated desmin filaments accumulated in the insoluble pellet, although their levels decreased in the cytosol (Fig. 5 I), suggesting a role for calpain-1 also in the normal turnover of desmin filaments. The sequence of events leading to desmin filament depolymerization in normal muscle, and the nature of the subsequent steps, which probably lead to the slower turnover of myofibrils, are important questions for future research.

Together, our studies implicate phosphorylation by GSK3-β as an initial key step in the selective depolymerization of desmin filaments by calpain-1, and the resulting loss of myofibrils, which is the defining feature of atrophy. Because GSK3-β and calpain-1 are key regulators of this process, their inhibition should be of major therapeutic promise for the treatment of numerous wasting conditions, ranging from prolonged bed rest to cancer-associated cachexia, by blocking protein breakdown and/or promoting protein synthesis and growth.

Materials and methods

Animal work
All animal experiments were consistent with Israel Council on Animal Experiments guidelines and the Institutional Regulations of Animal Care and Use. Specialized personnel provided mice care in the institutional animal facility. Muscle denervation was performed by sectioning the sciatic nerve on one limb; the contralateral leg served as a control. Muscles were dissected 3, 7, 10, or 14 d after denervation, and electroporation was performed on the day of denervation. In fasting (2 d) experiments, food was removed from cages on the fifth day after electroporation.

Antibodies, constructs, and materials
Plasmids encoding shRNA against Calpain-1, Trim32, and shLacz were cloned into pcDNA 6.2GW/EmGFP-miR vector using Invitrogen's BLOCK-iT RNAi expression vector kit (Cohen et al., 2012, 2014). Plasmid encoding HA-tagged GSK3-β-DN (K85A catalytically dead mutant; catalog number 14755) and GST-tagged GSK3-β encoding plasmid for bacterial expression (catalog number 15898) were a gift from J. Woodgett (Lunenfeld-Tanenbaum Research Institute Mount Sinai Hospital, Toronto, Ontario), GST-tagged GCN2 (GCN2-KD1-pGEX4T-1; catalog number 21876) was a gift from D. Ron (New York University School of Medicine, New York, NY; Harding et al., 2000), and all were purchased from Addgene. A plasmid encoding 6His-Calpain-1 was a gift from S. Hata (Tokyo Metropolitan Institute of Medical Science, Tokyo, Japan; Hata et al., 2012). Desmin antibodies were obtained from Abcam (ab8592, rabbit; images presented in Figs. 1 and S2), and from Developmental Studies Hybridoma Bank under the auspices of the National Institute of Child Health and Human Development (University of Iowa, Iowa City, IA): clone D3 (mouse) was deposited by D.A. Fischman (Cornell University Medical College, New York, NY; used in Fig. 5). Anti-puromycin antibody (MABE343, mouse) was from Millipore. Anti-actin (A2066, rabbit), β-catenin (AV14001, rabbit), GST (G7781, rabbit), and GAPDH (G8795, mouse) were from Sigma-Aldrich; anti-GSK3α/β (5676S, rabbit), phospho-GSK3α/β (8566, rabbit), phospho-PI3K (4228, rabbit), phospho-AKT (9275, rabbit), AKT (9272, rabbit), phospho-FoxO (9464, rabbit), calpain-1 (2556, rabbit), and calpain-2 (2539, rabbit) were from Cell Signaling; and anti–phospho-threonine/serine (PP2551, rabbit) was from ECM Biosciences. GSK3-β peptide inhibitor L803-mts (361546) was purchased from Calbiochem, and each mouse was injected i.p. with 400 nmol (0.3 mg per ~27–30-g mouse) twice on the first and then on the second day of fasting. Calcium green-1-AM was purchased from Thermo Fisher Scientific (C3011MP). The calpain specific substrate SLY-AMC was purchased from Sigma-Aldrich (S1153). Muscles from Calpain-1 knockout mice were provided by M. Baudry (Western University of Health Sciences, Pomona, CA).

In vivo transfection

In vivo electroporation experiments were performed in adult CD-1 male mice (~27–30 g). Plasmid DNA (20 µg) was injected into adult mouse TA muscles, and a mild electric pulse was applied using two electrodes (12 V, five pulses, 200-ms intervals). For fiber size analysis, muscle cross sections were fixed in 4% PFA and incubated in blocking solution (50 mg/ml BSA/TBS-T) for 20 min at room temperature, and fiber membrane was stained with a 1:50 dilution of laminin antibody (L9393, rabbit; Sigma-Aldrich) and a 1:1,000 dilution of Alexa Fluor 568–conjugated secondary antibody (A-11011, goat; Thermo Fisher Scientific), both antibodies diluted in blocking solution. Cross-sectional areas of at least 500 transfected (expressing GFP) and adjacent 500 nontransfected fibers in the same muscle section (10 µm) were measured using Imaris (Bitplane) software (n = 6 mice). Images were collected using a Nikon Ni-U upright fluorescence microscope with Plan Fluor 20× 0.5-NA objective lens and a Hamamatsu C8484-03 cooled CCD camera, at room temperature.

Fractionation of muscle tissue

Muscles were homogenized in lysis buffer (20 mM Tris, pH 7.2, 5 mM EGTA, 100 mM KCl, 1% Triton X-100, 1 mM PMSF, 10 mM sodium pyrophosphate, 3 mM benzamidine, 10 µg/ml leupeptin, 10 µg/ml aprotinin, 50 mM NaF, and 2 mM sodium orthovanadate) and incubated for 1 h at 4°C. After centrifugation at 6,000 g for 20 min at 4°C, the supernatant (i.e., soluble fraction) was stored at –80°C. The insoluble pellet was washed once with homogenization buffer and twice with suspension buffer (20 mM Tris, pH 7.2, 100 mM KCl, 1 mM DTT, and 1 mM PMSF), and after a final centrifugation at 6,000 g for 10 min at 4°C, the insoluble pellet (i.e., insoluble fraction containing myofibrils and desmin filaments) was resuspended in storage buffer (20 mM Tris, pH 7.2, 100 mM KCl, 1 mM DTT, and 20% glycerol) and kept at –80°C.

To isolate desmin filaments, the insoluble muscle pellet (40 µg) was resuspended in ice-cold extraction buffer (0.6 M KCl, 1% Triton X-100, 2 mM EDTA, 2 mM PMSF, 1× PBS, 10 µg/ml leupeptin, 3 mM benzamidine, 10 µg/ml aprotinin, 50 mM NaF, 2 mM sodium orthovanadate, and 10 mM sodium pyrophosphate) for 10 min on ice. After centrifugation at 6,000 g for 10 min at 4°C, the pellet was resuspended in 20 µl of 20 mM Tris, pH 7.5, supplemented with protein loading dye and DTT (50 mM), and 15 µl was analyzed by SDS-PAGE and immunoblotting.

Protein analysis

To determine the total content of myofibrils (Fig. 4, E and F), the protein concentration of insoluble myofibrillar pellet was determined using Bradford reagent and multiplied by the total volume of this fraction per muscle. To determine the effect of GSK3-β inhibition on myofibrillar components (Figs. 1 G and S1 B), equal amounts (2.5 µg) of isolated myofibrils were analyzed by SDS-PAGE and Coomassie blue staining. For immunoblotting, soluble (25 µg) or myofibrillar (2.5 µg) fractions were resolved by SDS-PAGE, transferred onto PVDF membranes, and immunoblotted with specific primary antibodies and secondary antibodies conjugated to HRP. Chemiluminescence signal was detected using ChemiDoc Imaging System (Bio-Rad).

Calpain activity assay

Calpain activity (Fig. 3, A–C) in 150 µg myofibrillar fraction was measured as the Ca^{2+}-dependent cleavage of 125 µM SLY-AMC, a calpain specific substrate, in reaction buffer (20 mM Tris-HCl, pH 7.5, 5 mM $CaCl_2$, and 1 mM DTT). After an incubation in the dark at 37°C for 3 h at 1,400 rpm, an endpoint fluorescence signal was measured using SpectraMax M5 plate reader (Molecular Devices). Data are expressed as relative fluorescent unit per milligram muscle protein.

Measurement of cellular Ca^{2+} levels in mouse skeletal muscle

To measure cellular free Ca^{2+} levels, we modified the previously published protocol (Sato et al., 1988). Gastrocnemius muscles were cut into thin strips of 2-mm width and 7-mm length using a razor blade and placed in 24-well plate containing PSS solution (136.9 mM NaCl, 5.4 mM KCl, 1 mM $MgCl_2$, 20 mM Hepes, 0.01 mM EDTA, and 5.5 mM D-glucose, pH 7.4), which was equilibrated with 100% O_2 for 15 min at RT. After incubation for 1 h at RT, muscles were transferred to PSS working solution (PSS solution supplemented with 1.5 mM $CaCl_2$, 0.5% Cremophor [C5135; Sigma-Aldrich] to increase dye solubility, and 10 µM calcium green-1-AM), and incubated at RT for 20 min. In control wells, muscles were incubated in PSS solution and 0.5% Cremophor without calcium green-1-AM. After incubation, muscles were washed in PSS solution and visualized under a Nikon Ni-U upright fluorescent microscope (excitation: 488 nm).

In vitro cleavage assay by calpain-1

Muscle pellets (30 µg) isolated from normal and atrophying muscles expressing shlacz, shCAPN1, or GSK3-β-DN (Fig. 5), were incubated with 6 µg purified 6His-Calpain-1 in reaction buffer (100 mM Hepes, 10 mM DTT, and 5 mM $CaCl_2$) at 30°C for the indicated time points (total reaction volume 50 µl). Negative control samples also contained 50 mM EGTA. Desmin cleavage by calpain-1 was determined by SDS-PAGE and immunoblotting using desmin and phospho-serine antibodies.

For phosphatase assay (Fig. 5 H), 30 µg of pellets from muscles expressing shCAPN1 during fasting were treated or left untreated with 50 U CIP (M0290S; BioLabs) in reaction buffer (50 mM Tris, pH 8, 100 mM NaCl, and 10 mM $MgCl_2$) and total reaction volume of 20 µl. A clear mobility shift in desmin can be observed in treated samples (Fig. 5 H, lanes 6–9). After 1-h incubation at 37°C and 1,000 rpm, samples were subjected to cleavage by calpain-1 as described above (total reaction volume 50 µl).

Purification of 6His-calpain-1

6His-tagged calpain-1 was purified from BL21 bacteria (OD 0.6) grown with 0.2 mM IPTG at 17°C overnight. After centrifugation (4000 g at 4°C for 20 min), the pellet was lysed with lysis buffer (50 mM NaH_2PO_4, 300 mM NaCl, and 10 mM imidazole) and a microfluidizer, and centrifuged at 10,000 g at 4°C for 20 min. The obtained supernatant was incubated with a nickel column for 1 h at 4°C, the column was washed twice with wash buffer (50 mM NaH_2PO_4, 300 mM NaCl, and 20 mM imidazole), and 6His-calpain-1 was eluted with elution buffer (50 mM NaH_2PO_4, 300 mM NaCl, and 250 mM imidazole). After dialysis against 50 mM Tris,

pH 7.6, overnight at 4°C, 1 mM DTT and 10% glycerol were added, and purified calpain-1 was stored at –80°C.

In vitro phosphorylation assay

Myofibrillar fractions (5 µg) from 3-d-denervated muscles expressing GSK3-β-DN were incubated with 500 ng GST-GSK3-β or GST-GCN2 in reaction buffer (40 mM Tris, pH 7.6, 20 mM MgCl$_2$, 250 µM DTT, 5 mM EGTA, and 2 mM ATP) for 30 min at 30°C. Negative control samples contained 50 mM EGTA or did not contain an enzyme. Desmin phosphorylation was analyzed by SDS-PAGE and immunoblotting.

Purification of GST-GSK3-β and GST-GCN2

GST-GSK3-β or GST-GCN2 were purified from BL21 bacteria (OD 0.6) grown with 0.3 mM IPTG at 17°C overnight. After centrifugation, (4,000 g at 4°C for 20 min), the pellet was lysed with buffer A (1× PBS and 1 mM PMSF) and a microfluidizer, and centrifuged at 10,000 g at 4°C for 20 min. The obtained supernatant was incubated with glutathione resin (resuspended in 1× PBS) for 1 h at 4°C. Then, the resin was washed three times with wash buffer (50 mM Tris, pH 7.6, 100 mM NaCl, and 1 mM DTT), and the GST-tagged enzymes were eluted with elution buffer (50 mM Tris, pH 8, and 10 mM reduced glutathione). After dialysis against 50 mM Tris, pH 7.6, overnight at 4°C, 1 mM DTT and 10% glycerol were added, and the purified enzymes were stored at –80°C.

In vivo measurement of protein synthesis rates

5 d after muscle electroporation, mice were deprived of food for 2 d, and 30 min before euthanasia, the mice were anesthetized and injected with puromycin (0.04 µmol/g body weight, i.p.). Exactly 25 min after injection, mice were sacrificed, and dissected TA muscles were snap-frozen in liquid nitrogen. Effects on protein synthesis rates were assessed by SDS-PAGE and immunoblotting using puromycin antibody.

Kinase-trap assay

To isolate the protein kinases having high affinity to desmin filaments, 30 µg of insoluble fraction (6,000 g pellet) and the corresponding soluble fractions (100 µg) from innervated and 3-d-denervated muscles were incubated with 2 mM AMP-PNP in reaction buffer (10 mM MgCl$_2$ and 1 mM DTT) for 1 h at 37°C. Then, samples were centrifuged at 3,000 g for 5 min at 4°C, and the pellet (containing desmin filaments and myofibrillar proteins) was washed twice in wash buffer (2 mM ATP, 20 mM Tris-HCl, pH 7.6, 20 mM KCl, 5 mM MgCl$_2$, and 1 mM DTT) and analyzed by mass spectrometry.

Protein identification by mass spectrometry

For mass spectrometry analysis, protein bands were excised from gel, reduced with 3 mM DTT in 100 mM ammonium bicarbonate (ABC; 60°C, 30 min), modified with 10 mM iodoacetamide in 100 mM ABC (in the dark, RT, 30 min), and digested in 10% acetonitrile and 10 mM ABC with modified trypsin (Promega) at a 1:10 enzyme-to-substrate ratio overnight at 37°C. The resulting peptides were desalted using C18 tips (Homemade stage tips, Empore), dried, and resuspended in 0.1% formic acid. The peptides were then resolved by reverse-phase chromatography

on 0.075 × 180-mm fused silica capillaries (J&W) packed with Reprosil reversed phase material (Dr. Maisch) and eluted with linear 60-min gradient of 5–28%, 15-min gradient of 28–95%, and 15 min at 95% acetonitrile with 0.1% formic acid in water at flow rates of 0.15 µl/min. Mass spectrometry was performed by Q Exactive plus mass spectrometer (Thermo Fisher Scientific) in positive mode using repetitively full MS scan followed by collision induced dissociation of the 10 most dominant ions selected from the first MS scan.

The mass spectrometry data were analyzed using Proteome Discoverer 1.4 software with Sequest (Thermo Fisher Scientific) and Mascot (Matrix Science) algorithms against mouse uniprot database with mass tolerance of 10 ppm for the precursor masses and 0.05 amu for the fragment ions. Minimal peptide length was set to six amino acids, and a maximum of two mis-cleavages was allowed. Peptide- and protein-level false discovery rates (FDRs) were filtered to 1% using the target-decoy strategy. Protein tables were filtered to eliminate the identifications from the reverse database and from common contaminants. Semiquantitation was done by calculating the peak area of each peptide based its extracted ion currents, and the area of the protein is the average of the three most intense peptides from each protein.

Quantitative real-time PCR

Total RNA was isolated from muscle using TRI reagent (T9424; Sigma-Aldrich) and served as a template for synthesis of cDNA by reverse transcription using qScript cDNA synthesis kit (95047-025; Quanta Biosciences). Real-time PCR was performed on mouse target genes using specific primers (Table S1) and the Perfecta SYBR Green qPCR kit (95073-012; Quanta Biosciences) according to the manufacturer's protocol.

Statistical analysis and image acquisition

All data are presented as means ± SEM. The statistical significance was accessed with the paired Student's *t* test. Muscle sections were imaged at room temperature with a Nikon Ni-U upright fluorescence microscope with Plan Fluor 20× 0.5-NA objective lens and a Hamamatsu C8484-03 cooled CCD camera. Image acquisition and processing was performed using Imaris software (Bitplane). Black-and-white images were processed with Adobe Photoshop CS5, version 12.1x64 software.

Online supplemental material

Fig. S1 shows that expression of GSK3-β-DN in normal muscle for 4 d does not induce muscle growth or protein synthesis and has no effect on desmin filament integrity or myofibril content. In addition, it includes Western Blot analysis of homogenates from GSK3-β-DN–expressing muscles showing increased Akt phosphorylation, which did not affect desmin or atrogene expression or rates of protein synthesis compared with shLacz control. Fig. S2 shows that GCN2 does not phosphorylate desmin filaments in vitro. Fig. S3 shows that inhibition of GSK3-β in denervated muscle (3 d) does not alter rates of protein synthesis. Fig. S4 includes RT-PCR analysis showing that inhibition of GSK3-β during atrophy does not induce desmin or myofibrillar actin. Table S1 contains a list of quantitative PCR primers and shRNA oligonucleotides that were used in the present study.

References

Adams, J.A. 2001. Kinetic and catalytic mechanisms of protein kinases. *Chem. Rev.* 101:2271–2290. https://doi.org/10.1021/cr000230w

Agnetti, G., V.L. Halperin, J.A. Kirk, K. Chakir, Y. Guo, L. Lund, F. Nicolini, T. Gherli, C. Guarnieri, C.M. Caldarera, et al. 2014. Desmin modifications associate with amyloid-like oligomers deposition in heart failure. *Cardiovasc. Res.* 102:24–34. https://doi.org/10.1093/cvr/cvu003

Albrecht, L.V., L. Zhang, J. Shabanowitz, E. Purevjav, J.A. Towbin, D.F. Hunt, and K.J. Green. 2015. GSK3- and PRMT-1–dependent modifications of desmoplakin control desmoplakin-cytoskeleton dynamics. *J. Cell Biol.* 208:597–612. https://doi.org/10.1083/jcb.201406020

Blunt, B.C., A.T. Creek, D.C. Henderson, and P.A. Hofmann. 2007. H2O2 activation of HSP25/27 protects desmin from calpain proteolysis in rat ventricular myocytes. *Am. J. Physiol. Heart Circ. Physiol.* 293:H1518–H1525. https://doi.org/10.1152/ajpheart.00269.2006

Bodine, S.C., E. Latres, S. Baumhueter, V.K. Lai, L. Nunez, B.A. Clarke, W.T. Poueymirou, F.J. Panaro, E. Na, K. Dharmarajan, et al. 2001. Identification of ubiquitin ligases required for skeletal muscle atrophy. *Science.* 294:1704–1708. https://doi.org/10.1126/science.1065874

Boucher, M.J., L. Selander, L. Carlsson, and H. Edlund. 2006. Phosphorylation marks IPF1/PDX1 protein for degradation by glycogen synthase kinase 3-dependent mechanisms. *J. Biol. Chem.* 281:6395–6403. https://doi.org/10.1074/jbc.M511597200

Cea, L.A., B.A. Cisterna, C. Puebla, M. Frank, X.F. Figueroa, C. Cardozo, K. Willecke, R. Latorre, and J.C. Sáez. 2013. De novo expression of connexin hemichannels in denervated fast skeletal muscles leads to atrophy. *Proc. Natl. Acad. Sci. USA.* 110:16229–16234. https://doi.org/10.1073/pnas.1312331110

Chen, F., R. Chang, M. Trivedi, Y. Capetanaki, and V.L. Cryns. 2003. Caspase proteolysis of desmin produces a dominant-negative inhibitor of intermediate filaments and promotes apoptosis. *J. Biol. Chem.* 278:6848–6853. https://doi.org/10.1074/jbc.M212021200

Chou, Y.H., W.L. Kuo, M.R. Rosner, W.J. Tang, and R.D. Goldman. 2009. Structural changes in intermediate filament networks alter the activity of insulin-degrading enzyme. *FASEB J.* 23:3734–3742. https://doi.org/10.1096/fj.09-137455

Cohen, S., J.J. Brault, S.P. Gygi, D.J. Glass, D.M. Valenzuela, C. Gartner, E. Latres, and A.L. Goldberg. 2009. During muscle atrophy, thick, but not thin, filament components are degraded by MuRF1-dependent ubiquitylation. *J. Cell Biol.* 185:1083–1095. https://doi.org/10.1083/jcb.200901052

Cohen, S., B. Zhai, S.P. Gygi, and A.L. Goldberg. 2012. Ubiquitylation by Trim32 causes coupled loss of desmin, Z-bands, and thin filaments in muscle atrophy. *J. Cell Biol.* 198:575–589. https://doi.org/10.1083/jcb.201110067

Cohen, S., D. Lee, B. Zhai, S.P. Gygi, and A.L. Goldberg. 2014. Trim32 reduces PI3K-Akt-FoxO signaling in muscle atrophy by promoting plakoglobin-PI3K dissociation. *J. Cell Biol.* 204:747–758. https://doi.org/10.1083/jcb.201304167

Cohen, S., J.A. Nathan, and A.L. Goldberg. 2015. Muscle wasting in disease: molecular mechanisms and promising therapies. *Nat. Rev. Drug Discov.* 14:58–74. https://doi.org/10.1038/nrd4467

Cole, A.R., and C. Sutherland. 2008. Measuring GSK3 expression and activity in cells. *Methods Mol. Biol.* 468:45–65. https://doi.org/10.1007/978-1-59745-249-6_4

Condeelis, J., and M. Vahey. 1982. A calcium- and pH-regulated protein from Dictyostelium discoideum that cross-links actin filaments. *J. Cell Biol.* 94:466–471. https://doi.org/10.1083/jcb.94.2.466

Conover, G.M., S.N. Henderson, and C.C. Gregorio. 2009. A myopathy-linked desmin mutation perturbs striated muscle actin filament architecture. *Mol. Biol. Cell.* 20:834–845. https://doi.org/10.1091/mbc.e08-07-0753

Cross, D.A., D.R. Alessi, P. Cohen, M. Andjelkovich, and B.A. Hemmings. 1995. Inhibition of glycogen synthase kinase-3 by insulin mediated by protein kinase B. *Nature.* 378:785–789. https://doi.org/10.1038/378785a0

Davis, T.A., and I.E. Karl. 1988. Resistance of protein and glucose metabolism to insulin in denervated rat muscle. *Biochem. J.* 254:667–675. https://doi.org/10.1042/bj2540667

Dechat, T., S.A. Adam, and R.D. Goldman. 2009. Nuclear lamins and chromatin: when structure meets function. *Adv. Enzyme Regul.* 49:157–166. https://doi.org/10.1016/j.advenzreg.2008.12.003

Doble, B.W., and J.R. Woodgett. 2003. GSK-3: tricks of the trade for a multi-tasking kinase. *J. Cell Sci.* 116:1175–1186. https://doi.org/10.1242/jcs.00384

Etlinger, J.D., R. Zak, D.A. Fischman, and M. Rabinowitz. 1975. Isolation of newly synthesised myosin filaments from skeletal muscle homogenates and myofibrils. *Nature.* 255:259–261. https://doi.org/10.1038/255259a0

Evenson, A.R., M.U. Fareed, M.J. Menconi, J.C. Mitchell, and P.O. Hasselgren. 2005. GSK-3β inhibitors reduce protein degradation in muscles from septic rats and in dexamethasone-treated myotubes. *Int. J. Biochem. Cell Biol.* 37:2226–2238. https://doi.org/10.1016/j.biocel.2005.06.002

Finol, H.J., D.M. Lewis, and R. Owens. 1981. The effects of denervation on contractile properties or rat skeletal muscle. *J. Physiol.* 319:81–92. https://doi.org/10.1113/jphysiol.1981.sp013893

Frame, S., and P. Cohen. 2001. GSK3 takes centre stage more than 20 years after its discovery. *Biochem. J.* 359:1–16. https://doi.org/10.1042/bj3590001

Galvez, A.S., A. Diwan, A.M. Odley, H.S. Hahn, H. Osinska, J.G. Melendez, J. Robbins, R.A. Lynch, Y. Marreez, and G.W. Dorn II. 2007. Cardiomyocyte degeneration with calpain deficiency reveals a critical role in protein homeostasis. *Circ. Res.* 100:1071–1078. https://doi.org/10.1161/01.RES.0000261938.28365.11

Geesink, G.H., S. Kuchay, A.H. Chishti, and M. Koohmaraie. 2006. Micro-calpain is essential for postmortem proteolysis of muscle proteins. *J. Anim. Sci.* 84:2834–2840. https://doi.org/10.2527/jas.2006-122

Geisler, N., and K. Weber. 1982. The amino acid sequence of chicken muscle desmin provides a common structural model for intermediate filament proteins. *EMBO J.* 1:1649–1656.

Geisler, N., and K. Weber. 1988. Phosphorylation of desmin in vitro inhibits formation of intermediate filaments; identification of three kinase A sites in the aminoterminal head domain. *EMBO J.* 7:15–20.

Goldspink, D.F. 1976. The effects of denervation on protein turnover of rat skeletal muscle. *Biochem. J.* 156:71–80. https://doi.org/10.1042/bj1560071

Goll, D.E., W.R. Dayton, I. Singh, and R.M. Robson. 1991. Studies of the alpha-actinin/actin interaction in the Z-disk by using calpain. *J. Biol. Chem.* 266:8501–8510.

Goll, D.E., V.F. Thompson, H. Li, W. Wei, and J. Cong. 2003. The calpain system. *Physiol. Rev.* 83:731–801. https://doi.org/10.1152/physrev.00029.2002

Gomes, M.D., S.H. Lecker, R.T. Jagoe, A. Navon, and A.L. Goldberg. 2001. Atrogin-1, a muscle-specific F-box protein highly expressed during muscle atrophy. *Proc. Natl. Acad. Sci. USA.* 98:14440–14445. https://doi.org/10.1073/pnas.251541198

Gulen, M.F., K. Bulek, H. Xiao, M. Yu, J. Gao, L. Sun, E. Beurel, O. Kaidanovich-Beilin, P.L. Fox, P.E. DiCorleto, et al. 2012. Inactivation of the enzyme GSK3α by the kinase IKKi promotes AKT-mTOR signaling pathway that mediates interleukin-1-induced Th17 cell maintenance. *Immunity.* 37:800–812. https://doi.org/10.1016/j.immuni.2012.08.019

Gumbiner, B.M. 2005. Regulation of cadherin-mediated adhesion in morphogenesis. *Nat. Rev. Mol. Cell Biol.* 6:622–634. https://doi.org/10.1038/nrm1699

Harding, H.P., I. Novoa, Y. Zhang, H. Zeng, R. Wek, M. Schapira, and D. Ron. 2000. Regulated translation initiation controls stress-induced gene ex-

pression in mammalian cells. *Mol. Cell.* 6:1099–1108. https://doi.org/10.1016/S1097-2765(00)00108-8

Hardt, S.E., H. Tomita, H.A. Katus, and J. Sadoshima. 2004. Phosphorylation of eukaryotic translation initiation factor 2Bepsilon by glycogen synthase kinase-3beta regulates beta-adrenergic cardiac myocyte hypertrophy. *Circ. Res.* 94:926–935. https://doi.org/10.1161/01.RES.0000124977.59827.80

Hata, S., M. Ueno, F. Kitamura, and H. Sorimachi. 2012. Efficient expression and purification of recombinant human m-calpain using an Escherichia coli expression system at low temperature. *J. Biochem.* 151:417–422. https://doi.org/10.1093/jb/mvs002

Hoeflich, K.P., J. Luo, E.A. Rubie, M.S. Tsao, O. Jin, and J.R. Woodgett. 2000. Requirement for glycogen synthase kinase-3beta in cell survival and NF-kappaB activation. *Nature.* 406:86–90. https://doi.org/10.1038/35017574

Huang, X., J. Li, D. Foster, S.L. Lemanski, D.K. Dube, C. Zhang, and L.F. Lemanski. 2002. Protein kinase C-mediated desmin phosphorylation is related to myofibril disarray in cardiomyopathic hamster heart. *Exp. Biol. Med. (Maywood).* 227:1039–1046. https://doi.org/10.1177/153537020222701113

Hudson, M.B., A.J. Smuder, W.B. Nelson, C.S. Bruells, S. Levine, and S.K. Powers. 2012. Both high level pressure support ventilation and controlled mechanical ventilation induce diaphragm dysfunction and atrophy. *Crit. Care Med.* 40:1254–1260. https://doi.org/10.1097/CCM.0b013e31823c8cc9

Huo, X., S. Liu, T. Shao, H. Hua, Q. Kong, J. Wang, T. Luo, and Y. Jiang. 2014. GSK3 protein positively regulates type I insulin-like growth factor receptor through forkhead transcription factors FOXO1/3/4. *J. Biol. Chem.* 289:24759–24770. https://doi.org/10.1074/jbc.M114.580738

Inagaki, M., Y. Nishi, K. Nishizawa, M. Matsuyama, and C. Sato. 1987. Site-specific phosphorylation induces disassembly of vimentin filaments in vitro. *Nature.* 328:649–652. https://doi.org/10.1038/328649a0

Inagaki, N., K. Tsujimura, J. Tanaka, M. Sekimata, Y. Kamei, and M. Inagaki. 1996. Visualization of protein kinase activities in single cells by antibodies against phosphorylated vimentin and GFAP. *Neurochem. Res.* 21:795–800. https://doi.org/10.1007/BF02532302

Jackman, R.W., and S.C. Kandarian. 2004. The molecular basis of skeletal muscle atrophy. *Am. J. Physiol. Cell Physiol.* 287:C834–C843. https://doi.org/10.1152/ajpcell.00579.2003

Jope, R.S., and G.V.W. Johnson. 2004. The glamour and gloom of glycogen synthase kinase-3. *Trends Biochem. Sci.* 29:95–102. https://doi.org/10.1016/j.tibs.2003.12.004

Kaufmann, E., K. Weber, and N. Geisler. 1985. Intermediate filament forming ability of desmin derivatives lacking either the amino-terminal 67 or the carboxy-terminal 27 residues. *J. Mol. Biol.* 185:733–742. https://doi.org/10.1016/0022-2836(85)90058-0

Kemp, C.M., W.T. Oliver, T.L. Wheeler, A.H. Chishti, and M. Koohmaraie. 2013. The effects of Capn1 gene inactivation on skeletal muscle growth, development, and atrophy, and the compensatory role of other proteolytic systems. *J. Anim. Sci.* 91:3155–3167. https://doi.org/10.2527/jas.2012-5737

Lazarides, E. 1978. The distribution of desmin (100 A) filaments in primary cultures of embryonic chick cardiac cells. *Exp. Cell Res.* 112:265–273. https://doi.org/10.1016/0014-4827(78)90209-4

Lazarides, E., and B.D. Hubbard. 1976. Immunological characterization of the subunit of the 100 A filaments from muscle cells. *Proc. Natl. Acad. Sci. USA.* 73:4344–4348. https://doi.org/10.1073/pnas.73.12.4344

Macqueen, D.J., L. Meischke, S. Manthri, A. Anwar, C. Solberg, and I.A. Johnston. 2010. Characterisation of capn1, capn2-like, capn3 and capn11 genes in Atlantic halibut (Hippoglossus hippoglossus L.): Transcriptional regulation across tissues and in skeletal muscle at distinct nutritional states. *Gene.* 453:45–58. https://doi.org/10.1016/j.gene.2010.01.002

Mavroidis, M., P. Panagopoulou, I. Kostavasili, N. Weisleder, and Y. Capetanaki. 2008. A missense mutation in desmin tail domain linked to human dilated cardiomyopathy promotes cleavage of the head domain and abolishes its Z-disc localization. *FASEB J.* 22:3318–3327. https://doi.org/10.1096/fj.07-088724

McClung, J.M., A.R. Judge, E.E. Talbert, and S.K. Powers. 2009. Calpain-1 is required for hydrogen peroxide-induced myotube atrophy. *Am. J. Physiol. Cell Physiol.* 296:C363–C371. https://doi.org/10.1152/ajpcell.00497.2008

Meijer, L., M. Flajolet, and P. Greengard. 2004. Pharmacological inhibitors of glycogen synthase kinase 3. *Trends Pharmacol. Sci.* 25:471–480. https://doi.org/10.1016/j.tips.2004.07.006

Mendez, M.G., S. Kojima, and R.D. Goldman. 2010. Vimentin induces changes in cell shape, motility, and adhesion during the epithelial to mesen-

chymal transition. *FASEB J.* 24:1838–1851. https://doi.org/10.1096/fj.09-151639

Milner, D.J., G. Weitzer, D. Tran, A. Bradley, and Y. Capetanaki. 1996. Disruption of muscle architecture and myocardial degeneration in mice lacking desmin. *J. Cell Biol.* 134:1255–1270. https://doi.org/10.1083/jcb.134.5.1255

Nelson, W.J., and P. Traub. 1983. Proteolysis of vimentin and desmin by the Ca2+-activated proteinase specific for these intermediate filament proteins. *Mol. Cell. Biol.* 3:1146–1156. https://doi.org/10.1128/MCB.3.6.1146

Plotkin, B., O. Kaidanovich, I. Talior, and H. Eldar-Finkelman. 2003. Insulin mimetic action of synthetic phosphorylated peptide inhibitors of glycogen synthase kinase-3. *J. Pharmacol. Exp. Ther.* 305:974–980. https://doi.org/10.1124/jpet.102.047381

Quélo, I., O. Akhouayri, J. Prud'homme, and R. St-Arnaud. 2004. GSK3 beta-dependent phosphorylation of the alpha NAC coactivator regulates its nuclear translocation and proteasome-mediated degradation. *Biochemistry.* 43:2906–2914. https://doi.org/10.1021/bi036256+

Rabinovich, E., A. Kerem, K.U. Fröhlich, N. Diamant, and S. Bar-Nun. 2002. AAA-ATPase p97/Cdc48p, a cytosolic chaperone required for endoplasmic reticulum-associated protein degradation. *Mol. Cell. Biol.* 22:626–634. https://doi.org/10.1128/MCB.22.2.626-634.2002

Raynaud, F., E. Fernandez, G. Coulis, L. Aubry, X. Vignon, N. Bleimling, M. Gautel, Y. Benyamin, and A. Ouali. 2005. Calpain 1-titin interactions concentrate calpain 1 in the Z-band edges and in the N2-line region within the skeletal myofibril. *FEBS J.* 272:2578–2590. https://doi.org/10.1111/j.1742-4658.2005.04683.x

Raynaud, F., C. Jond-Necand, A. Marcilhac, D. Fürst, and Y. Benyamin. 2006. Calpain 1-γ filamin interaction in muscle cells: a possible in situ regulation by PKC-α. *Int. J. Biochem. Cell Biol.* 38:404–413. https://doi.org/10.1016/j.biocel.2006.01.001

Rommel, C., S.C. Bodine, B.A. Clarke, R. Rossman, L. Nunez, T.N. Stitt, G.D. Yancopoulos, and D.J. Glass. 2001. Mediation of IGF-1-induced skeletal myotube hypertrophy by PI(3)K/Akt/mTOR and PI(3)K/Akt/GSK3 pathways. *Nat. Cell Biol.* 3:1009–1013. https://doi.org/10.1038/ncb1101-1009

Sagar, G.D.V., B. Gereben, I. Callebaut, J.-P. Mornon, A. Zeöld, W.S. da Silva, C. Luongo, M. Dentice, S.M. Tente, B.C.G. Freitas, et al. 2007. Ubiquitination-induced conformational change within the deiodinase dimer is a switch regulating enzyme activity. *Mol. Cell. Biol.* 27:4774–4783. https://doi.org/10.1128/MCB.00283-07

Sandri, M., C. Sandri, A. Gilbert, C. Skurk, E. Calabria, A. Picard, K. Walsh, S. Schiaffino, S.H. Lecker, and A.L. Goldberg. 2004. Foxo transcription factors induce the atrophy-related ubiquitin ligase atrogin-1 and cause skeletal muscle atrophy. *Cell.* 117:399–412. https://doi.org/10.1016/S0092-8674(04)00400-3

Sato, K., H. Ozaki, and H. Karaki. 1988. Changes in cytosolic calcium level in vascular smooth muscle strip measured simultaneously with contraction using fluorescent calcium indicator fura 2. *J. Pharmacol. Exp. Ther.* 246:294–300.

Seinfeld, J., N. Baudry, X. Xu, X. Bi, and M. Baudry. 2016. Differential activation of calpain-1 and calpain-2 following kainate-induced seizure activity in rats and mice. *eNeuro.* 3:1–12. https://doi.org/10.1523/ENEURO.0088-15.2016

Shen, J., P. Channavajhala, D.C. Seldin, and G.E. Sonenshein. 2001. Phosphorylation by the protein kinase CK2 promotes calpain-mediated degradation of IkappaBalpha. *J. Immunol.* 167:4919–4925. https://doi.org/10.4049/jimmunol.167.9.4919

Smith, I.J., S.H. Lecker, and P.O. Hasselgren. 2008. Calpain activity and muscle wasting in sepsis. *Am. J. Physiol. Endocrinol. Metab.* 295:E762–E771. https://doi.org/10.1152/ajpendo.90226.2008

Solomon, V., and A.L. Goldberg. 1996. Importance of the ATP-ubiquitin-proteasome pathway in the degradation of soluble and myofibrillar proteins in rabbit muscle extracts. *J. Biol. Chem.* 271:26690–26697. https://doi.org/10.1074/jbc.271.43.26690

Stamos, J.L., and W.I. Weis. 2013. The β-catenin destruction complex. *Cold Spring Harb. Perspect. Biol.* 5:a007898. https://doi.org/10.1101/cshperspect.a007898

Tang, H., K. Inoki, M. Lee, E. Wright, A. Khuong, A. Khuong, S. Sugiarto, M. Garner, J. Paik, R.A. DePinho, et al. 2014. mTORC1 promotes denervation-induced muscle atrophy through a mechanism involving the activation of FoxO and E3 ubiquitin ligases. *Sci. Signal.* 7:ra18. https://doi.org/10.1126/scisignal.2004809

Taylor, S.S., and A.P. Kornev. 2011. Protein kinases: evolution of dynamic regulatory proteins. *Trends Biochem. Sci.* 36:65–77. https://doi.org/10.1016/j.tibs.2010.09.006

Tidball, J.G., and M.J. Spencer. 2002. Expression of a calpastatin transgene slows muscle wasting and obviates changes in myosin isoform expression during murine muscle disuse. *J. Physiol.* 545:819–828. https://doi .org/10.1113/jphysiol.2002.024935

Valenta, T., G. Hausmann, and K. Basler. 2012. The many faces and functions of β-catenin. *EMBO J.* 31:2714–2736. https://doi.org/10.1038/emboj.2012.150

Verhees, K.J.P., A.M.W.J. Schols, M.C.J.M. Kelders, C.M.H. Op den Kamp, J.L.J. van der Velden, and R.C.J. Langen. 2011. Glycogen synthase kinase-3β is required for the induction of skeletal muscle atrophy. *Am. J. Physiol. Cell Physiol.* 301:C995–C1007. https://doi.org/10.1152/ajpcell.00520.2010

Viatour, P., E. Dejardin, M. Warnier, F. Lair, E. Claudio, F. Bureau, J.C. Marine, M.P. Merville, U. Maurer, D. Green, et al. 2004. GSK3-mediated BCL-3 phosphorylation modulates its degradation and its oncogenicity. *Mol. Cell.* 16:35–45. https://doi.org/10.1016/j.molcel.2004.09.004

Volodin, A., I. Kosti, A.L. Goldberg, and S. Cohen. 2017. Myofibril breakdown during atrophy is a delayed response requiring the transcription factor PAX4 and desmin depolymerization. *Proc. Natl. Acad. Sci. USA.* 114:E1375–E1384. https://doi.org/10.1073/pnas.1612988114

Watkins, G.R., N. Wang, M.D. Mazalouskas, R.J. Gomez, C.R. Guthrie, B.C. Kraemer, S. Schweiger, B.W. Spiller, and B.E. Wadzinski. 2012. Monoubiquitination promotes calpain cleavage of the protein phosphatase 2A (PP2A) regulatory subunit α4, altering PP2A stability and microtubule-associ-ated protein phosphorylation. *J. Biol. Chem.* 287:24207–24215. https://doi .org/10.1074/jbc.M112.368613

Wei, W., M.U. Fareed, A. Evenson, M.J. Menconi, H. Yang, V. Petkova, and P.O. Hasselgren. 2005. Sepsis stimulates calpain activity in skeletal muscle by decreasing calpastatin activity but does not activate caspase-3. *Am. J. Physiol. Regul. Integr. Comp. Physiol.* 288:R580–R590. https://doi.org/10 .1152/ajpregu.00341.2004

Woodgett, J.R. 1994. Regulation and functions of the glycogen synthase kinase-3 subfamily. *Semin. Cancer Biol.* 5:269–275.

Wyke, S.M., and M.J. Tisdale. 2006. Induction of protein degradation in skeletal muscle by a phorbol ester involves upregulation of the ubiquitin-proteasome proteolytic pathway. *Life Sci.* 78:2898–2910. https://doi.org/10 .1016/j.lfs.2005.11.014

Ye, X., H.M. Zhang, Y. Qiu, P.J. Hanson, M.G. Hemida, W. Wei, P.A. Hoodless, F. Chu, and D. Yang. 2014. Coxsackievirus-induced miR-21 disrupts cardiomyocyte interactions via the downregulation of intercalated disk components. *PLoS Pathog.* 10:e1004070. https://doi.org/10.1371/journal .ppat.1004070

Zorzato, F., P. Volpe, E. Damiani, D. Quaglino Jr., and A. Margreth. 1989. Terminal cisternae of denervated rabbit skeletal muscle: alterations of functional properties of Ca2+ release channels. *Am. J. Physiol.* 257:C504–C511. https://doi.org/10.1152/ajpcell.1989.257.3.C504